Supplemental Data

Mature *Drosophila* Meiosis I Spindles Comprise Microtubules of Mixed Polarity

Zhang-Yi Liang, Mark Andrew Hallen, and Sharyn Anne Endow

Supplemental Experimental Procedures

eb1-gfp Transgenic Flies

A P-element plasmid encoding DmEB1 [1] fused at the C terminus to S65T GFP [2] was constructed and injected into embryos to recover transgenic flies. *eb1-gfp #M6F1* was mapped to the X chromosome and tested in $eb1^{+}$ flies for mutant effects. Genetic tests showed slightly lower *eb1-gfp #M6F1* embryo viability (0.805, n=268, total=333) than wild-type controls (0.875, n=182, total=208) (χ^2=4.52, 1 d.f., p=0.03). *eb1-gfp #M6F1* females mated to $+/B^{S}Y$ males produced only one abnormal offspring (0.001, n=1, total=904), comparable to wild-type Ore R females (<0.001, n=0, total=1883) [3], indicating normal meiotic and mitotic chromosome distribution (χ^2=1.002, 1 d.f., p=0.32). Prometaphase to telophase midbody formation in *eb1-gfp #M6F1* cycle 10 embryos (279±6 s, n=16) was slightly longer than a wild-type transgenic line, *ncd-gfp #4121* (253±7 s, n=17) [4], or Ore R embryos (~252 s, n=3-11) [5], but the frequency of abnormal *eb1-gfp #M6F1* cycle 10 mitotic spindles (0.039, n=21, total=542) did not differ significantly from *ncd-gfp #4121* (0.061, n=20, total=327) (χ^2=2.76, 1 d.f., p=0.10). Centrosome-to-centrosome distance during *eb1-gfp #M6F1* cycle 10 interphase (9.9±0.1 μm, n=167), metaphase (12.5±0.1 μm, n=167) and anaphase (15.8±0.1 μm, n=167) was similar to *ncd-gfp #4121* (interphase, 9.5±0.2 μm, n=47; metaphase, 12.3±0.1 μm, n=47; anaphase, 15.7±0.1 μm, n=47) [4]. The genetic and cytological tests showed that *eb1-gfp #M6F1* is comparable to wild type in oocyte meiosis and mitosis in early embryos. A Western blot of *eb1-gfp #M6F1* females showed 4 major EB1 species and slightly lower (~1.1-1.4-fold) EB1-GFP than the corresponding endogenous EB1, indicating that the *eb1-gfp* transgene is not overexpressed compared to *eb1*.

EB1-GFP Particle Tracking and Fluorescence Flow Analysis

EB1 particle size was estimated by measuring particle fluorescence intensity with NIH ImageJ v 1.38x in time-lapse images of mature MI spindles of late stage 13 and stage 14 oocytes. Images were acquired at 0.72-0.80 s/frame and 0.1 x 0.1 μm pixel size using a Bio-Rad Radiance2100 confocal scanhead mounted on a Zeiss Axioskop 2 Plus microscope and LaserSharp 2000 software, a Plan-Apochromat 63x/1.4 NA oil immersion objective, and the 488-nm line of a 10 mW Kr-Ar laser. Fluorescence of particles of ≤5 x 5 pixels in the cytoplasm or spindle was measured and corrected for background by subtracting fluorescence in an

adjacent region of the cytoplasm or spindle devoid of visible particles. Particles in time-lapse sequences of MI spindles recorded at 0.38 to 2.5 s/frame were identified visually as moving and velocities were determined by measuring particle displacement over time in images from the sequences. Particle velocities were also determined from slopes of lines formed by moving particles in kymographs. Fluorescence flow was analyzed in image sequences acquired at ~1.55 s/image using the Bio-Rad confocal system described above and a Plan-Neofluar 40x/1.3 NA oil immersion objective. MI spindles were recorded at 0.05 x 0.05 μm pixel size and cycle 10 mitotic spindles from syncytial blastoderm embryos at 0.15 x 0.15 μm pixel size. Images were aligned manually and cropped before analysis using an ImageJ macro, *clearing*, to delete cytoplasm, centrosomes and astral microtubules. Fluorescence flow was analyzed using a MATLAB (The MathWorks) routine, *fluorescence_medians*, to determine the position over time of the fluorescence median in MI or mitotic half-spindles.

FRAP Assays

MI spindle assays were performed at 22-25ºC using a Zeiss LSM 510 confocal microscope and LSM 510 software, a Plan-Apochromat 63x/1.4 NA oil immersion objective, and the 488-nm line of a 30 mW Ar laser set at 75% power, as described [6]. Three prebleach images were collected at zoom 3, three bleach scans were performed at high laser power (ROI radius, w=0.55 μm), and 247 (EB1-GFP) or 397 (GFP-α-tubulin) recovery images were recorded at ~94 ms/image at low laser power (1%). Fluorescence intensity was measured in ImageJ in ROIs of w=0.26 and 0.5 μm centered in the bleach spot and tracked manually if the spindle moved. Values were normalized to the first prebleach image, averaged with data from 10-15 assays, corrected for fluorescence loss during imaging, and plotted versus time. The large and small ROIs showed overlapping recovery curves, indicating that recovery was dominated by binding interactions rather than diffusion. The data did not fit well to a single-state binding-dominant model, but showed a good fit to a two-state model. Data for the large and small ROIs were fit concurrently [6] using the MATLAB routine, *leasqr.m* [7], to a two-state binding-dominant model [8], $frap(t) = R(1 - C_{eq,fast}e^{-k_{off,fast}} - C_{eq,slow}e^{-k_{off,slow}})$, where C_{eq} denotes the fraction of protein bound at equilibrium in each binding state, R is the fluorescence at $t=\infty$, and k_{off} is the dissociation rate constant for each state. The pseudo-first order binding rate constant for each state was calculated by $k^*_{on}=(C_{eq}\ k_{off})/(1 - C_{eq,fast} - C_{eq,slow})$ and the half-time of recovery by $t_{1/2}=ln2/k_{off}$. Ninety-five percent confidence intervals were calculated from the parameter variances returned by the *leasqr.m* routine and are given as error estimates in Tables S1 and S2. Assays of MI spindles in taxol-treated oocytes were performed in the same way, except that oocytes were from females starved for 24±1 h, then fed 10 μM taxol in 1% sucrose for 48±3 h in the dark. Assays of mitotic spindles from cycle 10 embryos were with two ROIs (w=1.75 μm and 1.3 μm) and zoom 1, instead of zoom 3.

FLIP Assays

MI spindle assays were performed using the Zeiss LSM 510 confocal microscope above at 75% laser power by iteratively imaging at 1% power and bleaching at high power in a rectangular ROI (0.8 μm x 3.5 μm) at the equator or pole in cycles of 3 images + 1 bleach ≈ 352 ms for 300 frames (EB1-GFP, ~35 s) or 400 frames (GFP-α-tubulin, ~47 s) at zoom 3. Fluorescence was measured with ImageJ in an ROI (0.8 μm x 0.8 μm) at the unbleached pole or equator 3 μm from the bleached region; spindles in which the bleach ROI moved were excluded. Values were normalized to the first image, averaged with data from 8-15 assays, corrected for fluorescence loss during imaging, and fit using Kaleidagraph (Synergy Software) to a first-order exponential decay equation, $flip(t)=m3+m2\ e^{-m1*t}$, where $m1=k_{flip}$ (s^{-1}), *m2*=fraction of fluorescence lost during the assay, and *m3*=fluorescence at $t=\infty$. Assays of MI spindles in taxol-treated oocytes were performed in the same way, except that oocytes were from females fed taxol for 48±3 h, as described above. For assays of cycle 10 mitotic spindles, an ROI of 0.8 μm x 9.0 μm was bleached at zoom 1, cycles of 3 images + 1 bleach ≈ 368 ms were repeated for 400 frames (~49 s), and 300 frames were analyzed (~36 s) in an ROI of 0.86 μm x 3.14 μm.

Supplemental References

1. Rogers, S.L., Rogers, G.C., Sharp, D.J., and Vale, R.D. (2002). *Drosophila* EB1 is important for proper assembly, dynamics, and positioning of the mitotic spindle. J. Cell Biol. *158*, 873-884.
2. Heim, R., Cubitt, A.B., and Tsien, R.Y. (1995). Improved green fluorescence. Nature *373*, 663-664.
3. Endow, S.A., and Komma, D.J. (1997). Spindle dynamics during meiosis in *Drosophila* oocytes. J. Cell Biol. *137*, 1321-1336.
4. Sciambi, C.J., Komma, D.J., Sköld, H.N., Hirose, K., and Endow, S.A. (2005). A bidirectional kinesin motor in live *Drosophila* embryos. Traffic *6*, 1036-1046.
5. Foe, V.E., and Alberts, B.M. (1983). Studies of nuclear and cytoplasmic behaviour during the five mitotic cycles that precede gastrulation in *Drosophila* embryogenesis. J. Cell Sci. *61*, 31-70.
6. Hallen, M.A., Ho, J., Yankel, C.D., and Endow, S.A. (2008). Fluorescence recovery kinetic analysis of γ-tubulin binding to the mitotic spindle. Biophys. J. *95*, 3048-3058.
7. Shrager, R., Jutan, A., and Muzic, R. (1994). *leasqr.m*. http://octave.sourceforge.net/doc/f/leasqr.html
8. Sprague, B.L., Pego, R.L., Stavreva, D.A., and McNally, J.G. (2004). Analysis of binding reactions by fluorescence recovery after photobleaching. Biophys. J. *86*, 3473-3495.

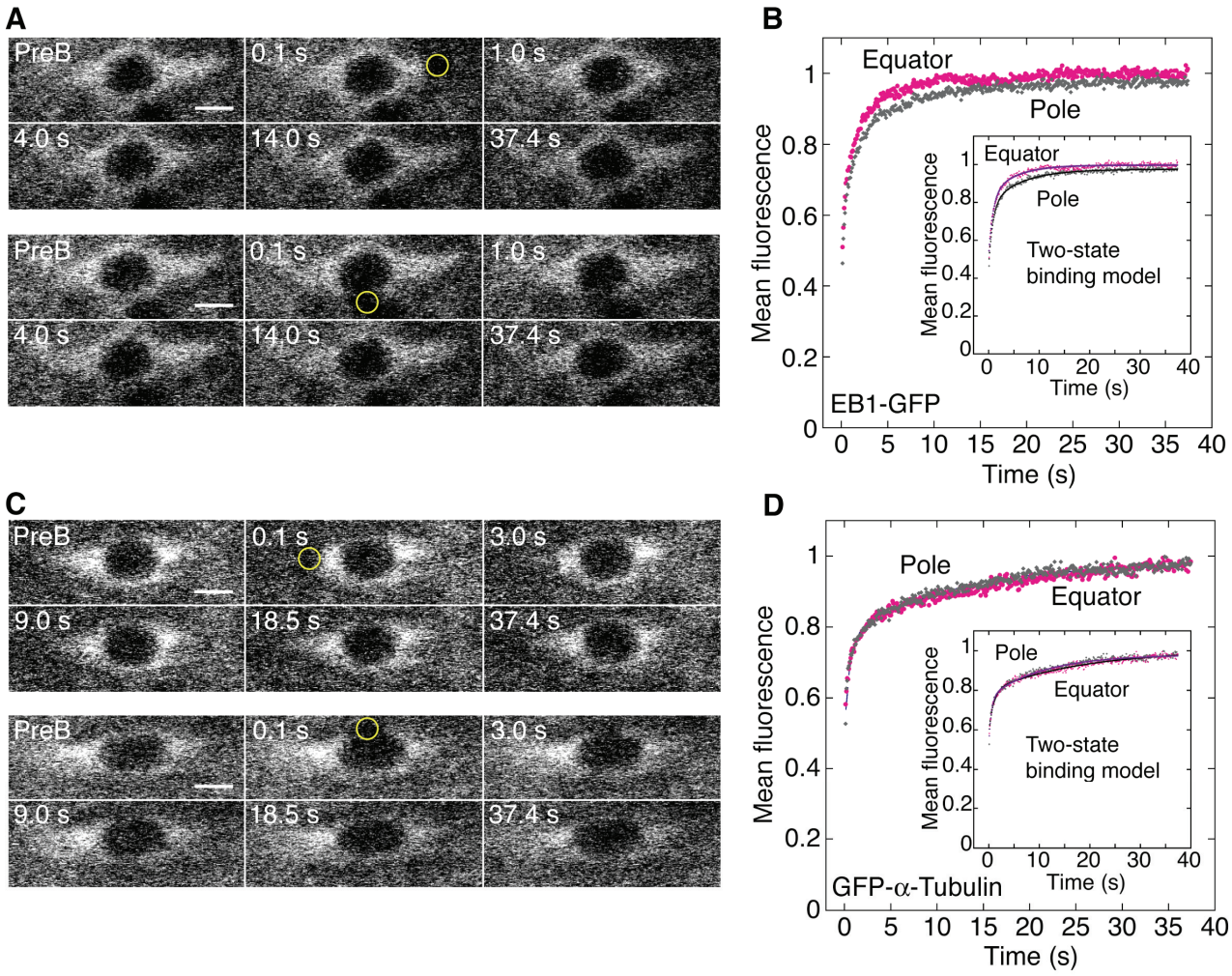

Figure S1. EB1 and α-tubulin FRAP Assays in Taxol-Treated Oocyte MI Spindles

(A) EB1-GFP FRAP assay at an MI spindle pole (top) or equator (bottom) of an oocyte treated with taxol (48 h). ROI radius, *w*=0.55 μm (yellow circle). PreB, prebleach. Bars, 2 μm.

(B) Mean recovery data (*w*=0.5 μm) for the pole (grey, *n*=13) and equator (magenta, *n*=13) vs time. Inset, fits to a two-state binding model.

(C) GFP-α-tubulin FRAP assay at an MI spindle pole (top) or equator (bottom) of an oocyte treated with taxol (48 h). Bars, 2 μm.

(D) Mean recovery data (*w*=0.5 μm) for the pole (grey, *n*=15) and equator (magenta, *n*=15) vs time. Inset, fits to a two-state binding model.

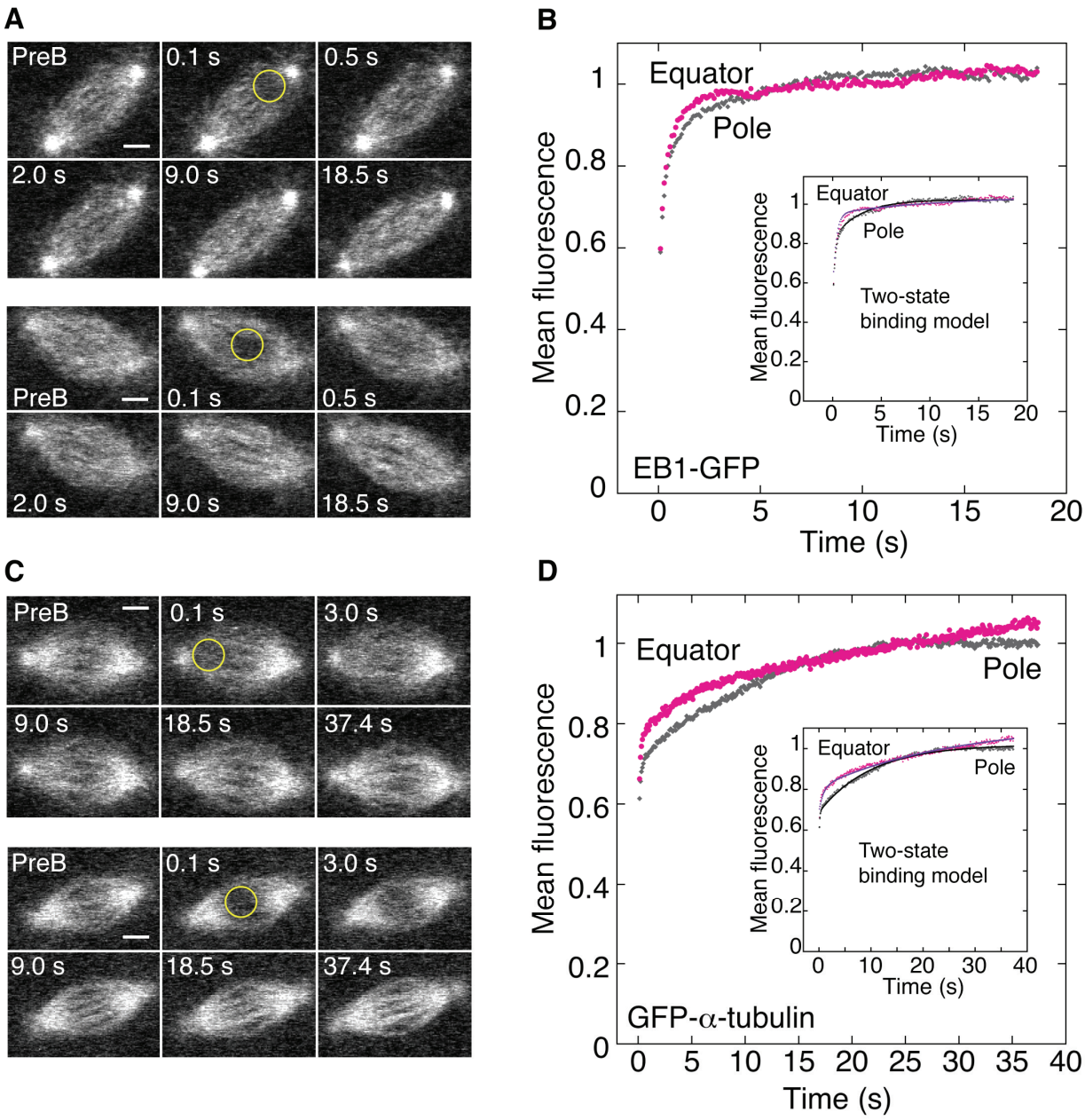

Figure S2. EB1 and α-tubulin FRAP Assays in Mitotic Spindles

(A) EB1-GFP FRAP assay at a cycle 10 mitotic spindle pole (top) or equator (bottom). ROI, *w*=1.75 µm (yellow circle). PreB, prebleach. Bars, 3 µm.

(B) Mean recovery data (*w*=1.75 µm) at the pole (grey, *n*=9) and equator (magenta, *n*=11) vs time. Inset, fits to a two-state binding model.

(C) GFP-α-tubulin FRAP assay at a cycle 10 mitotic spindle pole (top) or equator (bottom). PreB, prebleach. Bars, 3 µm.

(D) Mean recovery data (*w*=1.75 µm) at the pole (grey, *n*=13) and equator (magenta, *n*=14) vs time. Inset, fits to a two-state binding model.

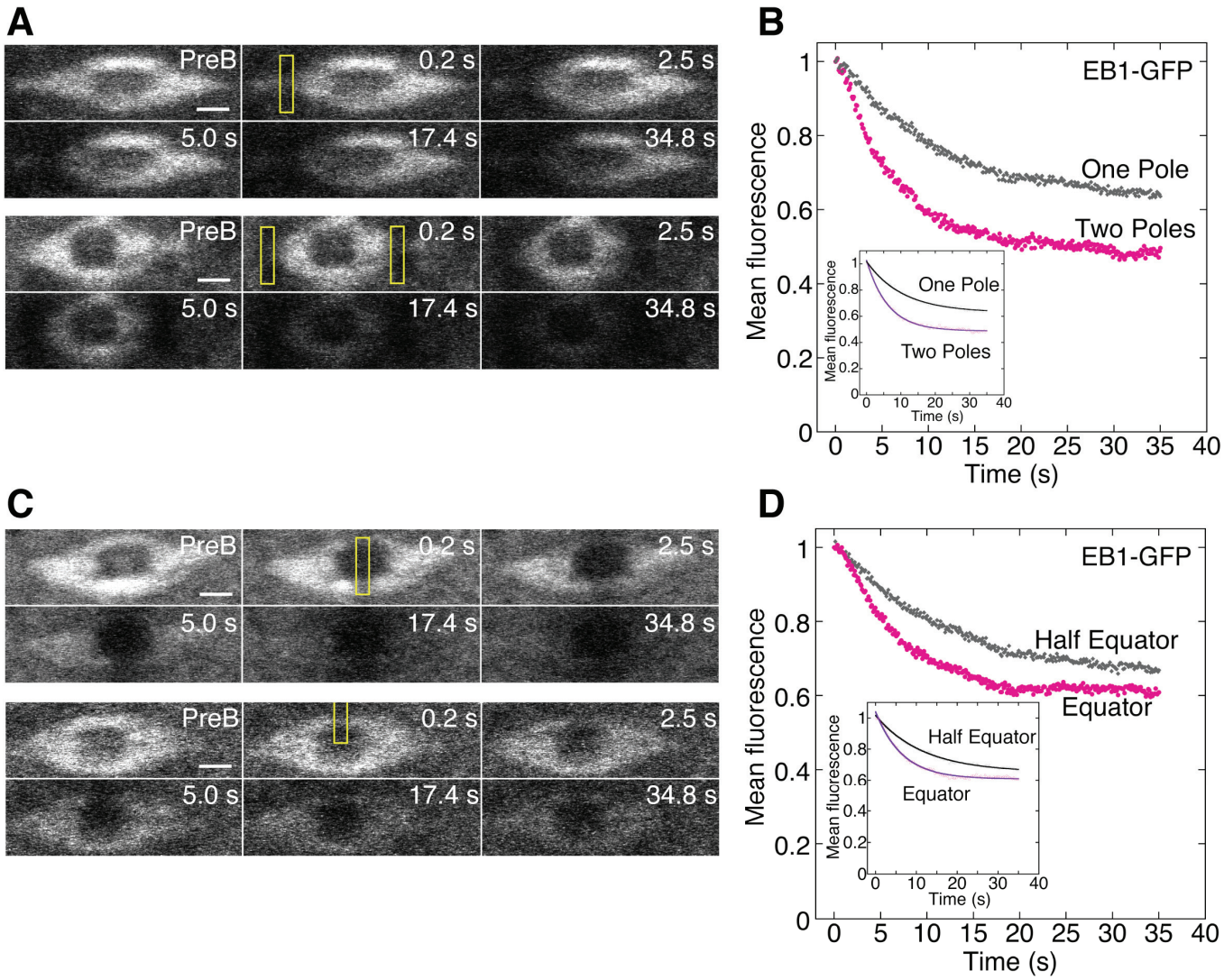

Figure S3. EB1 FLIP Assays at Two Poles or a Half Equator of the Oocyte MI Spindle

(A) EB1-GFP FLIP assay at one (top) or two (bottom) MI spindle poles. ROIs=0.8 µm x 3.5 µm (yellow rectangles). PreB, prebleach. Bars, 2 µm.

(B) Mean fluorescence loss at the equator vs time upon bleaching one (grey, n=14) or two (magenta, n=12) poles. Inset, fits to a first-order exponential decay equation with only every third data point shown.

(C) EB1-GFP FLIP assay at an MI spindle equator (top) or half-equator (bottom). Bars, 2 µm.

(D) Mean fluorescence loss at the poles vs time upon bleaching a half-equator (grey, n=20) or entire equator (magenta, n=15). Inset, fits to a first-order exponential equation with only every third data point shown.

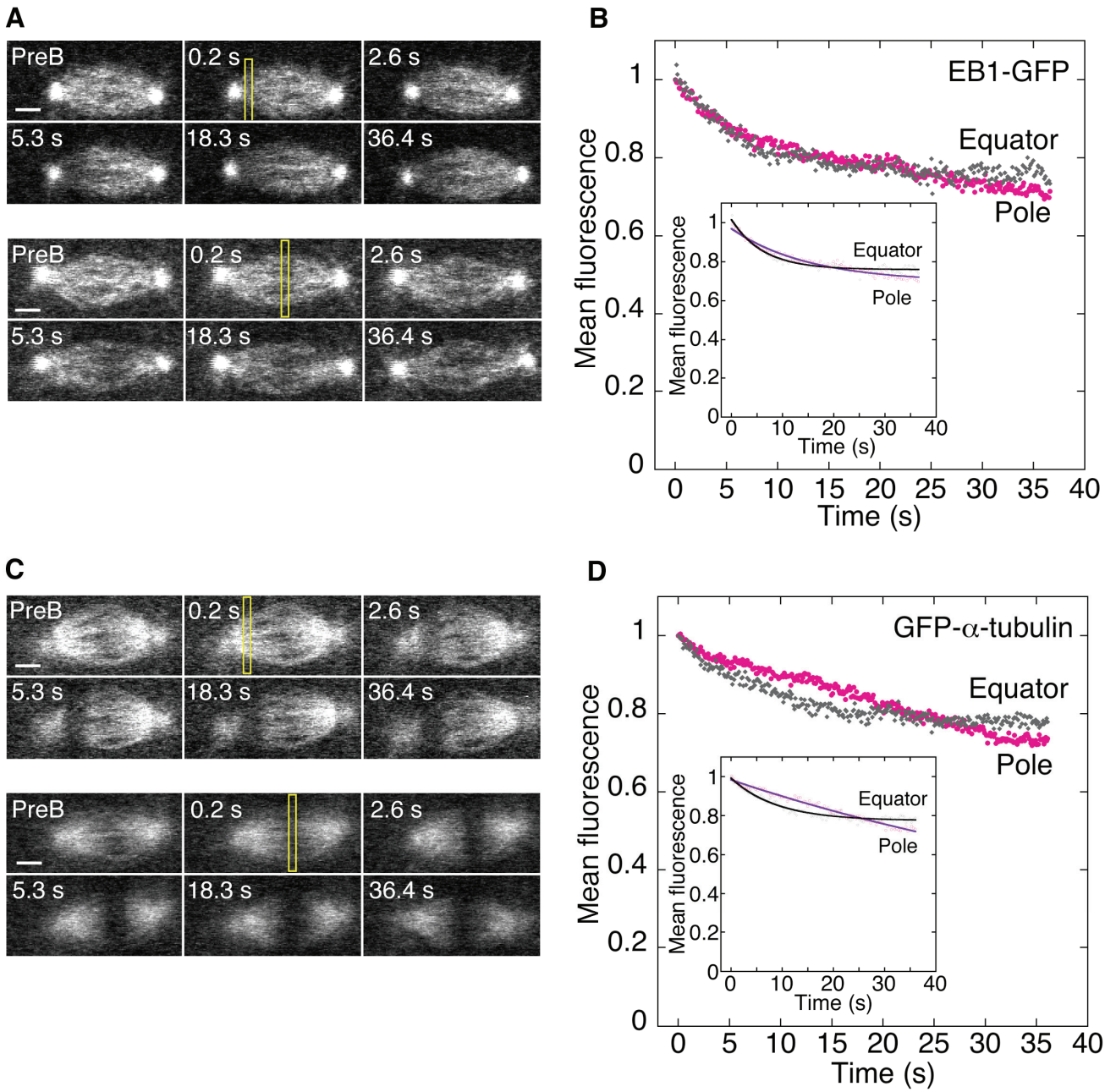

Figure S4. EB1 and α-tubulin FLIP Assays in Mitotic Spindles

(A) EB1-GFP FLIP assay at a cycle 10 mitotic spindle pole (top) or equator (bottom). ROI=0.8 µm x 9.0 µm (yellow rectangle). PreB, prebleach. Bars, 3 µm.

(B) Mean fluorescence loss at the pole (magenta, *n*=8) or equator (grey, *n*=8) vs time. Inset, fits to a first-order exponential decay equation with only every third point shown.

(C) GFP-α-tubulin FLIP assay at a cycle 10 mitotic spindle pole or equator. PreB, prebleach. Bars, 3 µm.

(D) Mean fluorescence loss at the pole (magenta, *n*=9) or equator (grey, *n*=9) vs time. Inset, fits to a first-order exponential equation with only every third point shown.

Table S1. FRAP Rate Constants

	Pole					Equator				
	Fast k_{off} (s^{-1})	Slow k_{off} (s^{-1})	Fast k^*_{on} (s^{-1})	Slow k^*_{on} (s^{-1})	*n*	Fast k_{off} (s^{-1})	Slow k_{off} (s^{-1})	Fast k^*_{on} (s^{-1})	Slow k^*_{on} (s^{-1})	*n*
EB1-GFP										
MI spindle										
No taxol	3.5±0.7	0.45±0.04	2.9±0.8	0.25±0.05	10	2.6±0.5	0.51±0.06	2.4±0.7	0.4±0.1	11
Taxol (48 h)	1.2±0.1	0.16±0.01	0.8±0.1	0.066±0.008	13	1.2±0.2	0.20±0.02	0.8±0.1	0.07±0.01	13
Mitotic spindle	5.2±0.5	0.35±0.02	4.6±0.7	0.16±0.01	9	2.8±0.3	0.09±0.04	1.9±0.3	0.014±0.006	11
GFP-α-Tub										
MI spindle										
No taxol	1.0±0.1	0.080±0.005	0.53±0.07	0.051±0.004	12	1.0±0.1	0.059±0.003	0.52±0.08	0.072±0.004	12
Taxol (48 h)	1.9±0.3	0.093±0.006	0.9±0.2	0.038±0.003	15	1.1±0.1	0.054±0.006	0.41±0.06	0.019±0.002	15
Mitotic spindle	9±3	0.099±0.002	3±2	0.065±0.008	13	1.2±0.2	0.039±0.003	0.22±0.04	0.018±0.001	14

Values from concurrent fits of data from two different-sized bleach spots to a two-state binding-dominant model for FRAP recovery; fits to data from only one bleach spot for taxol. Mean±95% confidence interval from the curve fit.

Table S2. FRAP Kinetic Parameters

	Pole				Equator			
	Fast $t_{1/2}$ (*s*)	Slow $t_{1/2}$ (*s*)	Slow C_{eq}	*R*	Fast $t_{1/2}$ (*s*)	Slow $t_{1/2}$ (*s*)	Slow C_{eq}	*R*
EB1-GFP								
MI spindle								
No taxol	0.20±0.04	1.6±0.2	0.23±0.02	0.99	0.26±0.05	1.4±0.2	0.27±0.04	1.01
Taxol (48 h)	0.56±0.05	4.3±0.3	0.20±0.01	0.975±0.002	0.57±0.07	3.4±0.4	0.17±0.02	0.997±0.002
Mitotic spindle	0.13±0.01	1.97±0.09	0.193±0.006	1.04	0.24±0.02	8±3	0.087±0.009	1.03
GFP-α-Tub								
MI spindle								
No taxol	0.68±0.07	8.7±0.5	0.294±0.007	0.91	0.71±0.08	11.7±0.6	0.442±0.005	1.02
Taxol (48 h)	0.36±0.05	7.5±0.5	0.219±0.006	0.980±0.003	0.62±0.07	13±1	0.205±0.005	1.004±0.009
Mitotic spindle	0.07±0.02	7.0±0.1	0.325±0.002	1.01	0.57±0.09	18±1	0.275±0.005	1.12

Values calculated from concurrent fits of data from two different-sized bleach spots to a two-state binding-dominant model for FRAP recovery; fits to data from one bleach spot for taxol. Mean±95% confidence interval from the curve fit.

Table S3. FLIP Rate Constants

	Bleach pole Monitor equator k_{FLIP} (s^{-1})	Bleach equator Monitor pole k_{FLIP} (s^{-1})
EB1-GFP		
MI spindle		
No taxol	0.095±0.001 (n=14)	0.153±0.002 (n=15)
Taxol (48 h)	0.0438±0.0009 (n=13)	0.0789±0.0009 (n=12)
Two poles	0.160±0.002 (n=12)	
Half-equator		0.086±0.001 (n=20)
Mitotic spindle	0.167±0.005 (n=8)	0.066±0.003 (n=8)
GFP-α-Tub		
MI spindle		
No taxol	0.043±0.001 (n=8)	0.077±0.001 (n=8)
Taxol (48 h)	0.045±0.001 (n=8)	0.064±0.001 (n=10)
Mitotic spindle	0.112±0.003 (n=9)	0.011±0.002 (n=9)

Values from curve fits to a first-order exponential decay equation; mean±SEM.